ASM Sc. J., 19, 2024

https://doi.org/10.32802/asmscj.2023.1589

Anharmonic Thermal Expansion Coefficient of Crystalline Iron

T.S. Tien[1*], N.T.M. Thuy[1], V.T.K. Lien[1], B.Q. Thanh[1], N.T.V. Chinh[2], H.V. Yen[3], N.C. Toan[4] and N.B. Trung[4]

[1]*Department of Basic Sciences, University of Fire Prevention & Fighting, Hanoi 120602, Vietnam*

[2]*Institute of Science and Technology, TNU-University of Sciences, Thai Nguyen 251580, Vietnam*

[3]*Department of Basic Sciences, Artillery Officer School, Hanoi 154210, Vietnam*

[4]*Department of Physics, VNU University of Science, Hanoi 120602, Vietnam*

The anharmonic thermal expansion (TE) coefficient of crystalline iron (Fe) has been calculated and analysed in the temperature-dependent. The thermodynamic parameters of the crystal lattice are derived from the influence of the thermal vibrations of all atoms. The calculation model is developed from the correlated Einstein model and quantum-statistical perturbation theory using the anharmonic effective potential. The obtained expression of the temperature-dependent TE coefficient of Fe is an explicit form. The numerical results of Fe agree well with those obtained from the experiments at various temperatures in the range from 0 K to 900 K. The obtained results show that the present model is efficient in investigating the TE coefficient of Fe.

Keywords: thermal expansion coefficient; crystalline iron; anharmonic correlated Einstein model

I. INTRODUCTION

Nowadays, accurate information about the temperature-dependent thermal expansion (TE) coefficient of metals is necessary and important in engineering physics (Yokoyama, 2019), especially for metallurgy and mechanics. It is because many dynamic properties of metals can be defined from their anharmonic TE coefficient (Fornasini *et al.*, 2017). Moreover, this coefficient determines the compatibility of the component metals and the deformation of the alloys under the influence of temperature change (Stern *et al.*, 1980). Like the compressibility and heat capacity, the anharmonic TE coefficient of metals can be measured experimentally with high precision and is one of the independent thermodynamic properties (Vila *et al.*, 2018). However, the influence of thermal vibrations changes the interatomic distance of atoms and their positions (Lee *et al.*, 1981). This influence causes anharmonic effects and thermal disorders in the crystal lattice, so the increasing temperature is sensitive to the anharmonic TE coefficient (Eisenberger & Brown, 1979), as seen in Figure 1.

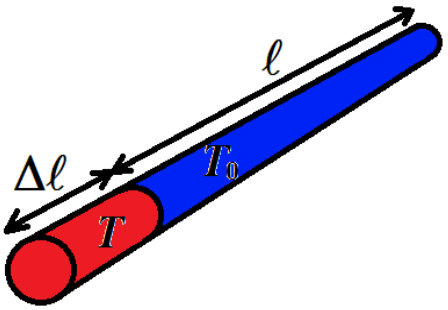

Figure 1. Thermal expansion of metal with a change in temperature.

In recent years, crystalline iron (Fe) having a body-centred cubic (BCC) structure accounts for over 90% of worldwide metal production (Emsley, 2011). Iron is the most widely used of all the metals because it is often used to create steel in civil engineering and manufacturing, such as bridges and aircraft, structural elements for buildings, hulls of ships and vehicles, and other machine tools (Smith & Hashemi, 2006; Tien, 2023). The experimental TE coefficient of Fe was measured by Dunn (2016), Landsberg (2018), and Hwang

*Corresponding author's e-mail: tongsytien@yahoo.com

(1972). However, there is still no effective theoretical model to calculate and analyse the anharmonic TE coefficient of Fe.

Meanwhile, a quantum anharmonic correlated Einstein (QACE) model has been used to effectively treat the anharmonic TE coefficient of metals (Hung *et al.*, 2017a; 2017b). This model has the advantage of investigating the anharmonic TE coefficient of crystals because the obtained expressions are explicit and are valid even in the low temperature (LT) region (Tien, 2020a; 2022). Therefore, calculating and analysing the anharmonic TE coefficient of Fe based on the QACE model will be a necessary addition to thermodynamic property investigations of Fe.

II. FORMALISM AND METHOD

A. Formalism

Normally, the TE coefficient characterises the net thermal expansion and can be determined by (Hung *et al.*, 2017b; Ho & Taylor, 1998; Tien, 2023):

$$\alpha_T(T) = \frac{d\ell}{\ell dT} = \frac{d\langle r\rangle}{\langle r\rangle dT} = \frac{d\langle r\rangle}{r_0 dT} \quad , \tag{1}$$

where T is the absolute temperature, ℓ is a particular length measurement, $\langle\ \rangle$ denotes the thermal average that can be calculated via true radial pair distribution (RPD) function using the statistical density matrix, and r_0 and r are the equilibrium and instantaneous atomic distances, respectively.

Usually, $\langle r\rangle$ describes the variance of real RPD function and can be presented in terms of the powerful moment of real RPD function (Tröger *et al.*, 1994), so the TE coefficient is rewritten as:

$$\alpha_T(T) = \frac{d\left(r_0 + \langle x\rangle\right)}{r_0 dT} = \frac{d\langle x\rangle}{r_0 dT} = \frac{d\sigma^{(1)}}{r_0 dT}, \tag{2}$$

where $\sigma^{(1)} = \langle x\rangle$ is the first cumulant in the cumulant expansion approach of the extended X-ray absorption fine structure (EXAFS) theory.

The general expression of the temperature-dependent EXAFS cumulant in the QACE model was calculated by Tien (2020). Still, the anharmonic TE coefficient of Fe has not yet been investigated in the temperature-dependent. Therefore, we extend this model to determine the temperature-dependent TE coefficient of Fe.

One usually considers an anharmonic effective (AE) potential (Hung & Rehr, 1997) to determine the thermodynamic parameters of crystals. If ignoring the constant contribution and extending to the third order (Yokoyama *et al.*, 1996), this potential is written in the form:

$$V_{eff}(x) = \frac{1}{2}k_{eff}x^2 - k_{an}x^3,\ x = r - r_0, \tag{3}$$

where x is the displacement, k_{eff} is the effective force constant, and k_{an} is the anharmonicity force constant.

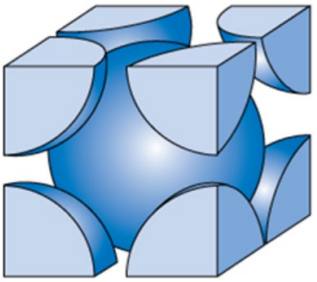

Figure 2. The BCC structural model of Fe.

The BCC structural model of Fe is illustrated in Figure 2. In the structure of Fe, it has similar atoms at one centre and eight corners of a cube, so each atom has a mass of m and each unit cell contains two atoms (Simon, 2013).

B. Method

The AE potential of Fe can be calculated via the Morse potential that describes the pair interaction potential of atoms (Girifalco & Weizer, 1959). Use of this structural characteristic, the AE potential of Fe is defined as follows (Tien, 2022):

$$V_{eff}(x) = \frac{11}{6}D\alpha^2x^2 - \frac{3}{4}D\alpha^3x^3, \tag{4}$$

where α is the width of Morse potential and D is the dissociation of Morse potential.

Comparing Eq. (3) with Eq. (4), the local force constants k_{eff} and k_{an} are deduced as follows:

$$k_{eff} = \frac{11}{3}D\alpha^2, \quad k_{an} = \frac{3}{4}D\alpha^3, \tag{5}$$

The QACE model (Tien, 2020a) was developed from the correlated Einstein model (Sevillano *et al.*, 1979) based on the first-order perturbation theory (Yokoyama *et al.*, 1996) and AE potential (Hung & Rehr, 1997). In the crystal lattice,

the atomic thermal vibrations of Fe are characterised by the correlated Einstein frequency ω_E and temperature θ_E (Tien, 2022).

Substituting the obtained local force constants k_{eff} in Eq. (5) into the general expression of these parameters (Tien, 2022), the correlated Einstein frequency and temperature of Fe are obtained as follows:

$$\omega_E = \sqrt{\frac{k_{eff}}{\mu}} = \alpha\sqrt{\frac{22D}{3m}}, \theta_E = \frac{\hbar\omega_E}{k_B} = \frac{\hbar\alpha}{k_B}\sqrt{\frac{22D}{3m}}, \quad (6)$$

where $\hbar$ is the reduced Planck constant and k_B is the Boltzmann constant.

Substituting the obtained local force constants k_{eff} and k_{an} in Eq. (5) into the general moment expression $\langle x \rangle$ (Tien, 2020a), the temperature-dependent EXAFS cumulant of Fe is obtained in the form as:

$$\sigma^{(1)} = \langle x \rangle = \frac{3\hbar\omega_E k_{an}}{2k_{eff}^2}\left(\frac{e^{\hbar\omega_E/k_BT}+1}{e^{\hbar\omega_E/k_BT}-1}\right) = \frac{81\hbar\omega_E}{968D\alpha}\left(\frac{e^{\hbar\omega_E/k_BT}+1}{e^{\hbar\omega_E/k_BT}-1}\right), \quad (7)$$

Substituting the obtained temperature-dependent EXAFS cumulant into Eq. (2) to calculate the temperature-dependent TE coefficient of Fe, we obtain the following results:

$$\alpha_T(T) = \frac{81\hbar^2\omega_E^2}{484D\alpha r_0 k_B T^2}\cdot\frac{e^{\hbar\omega_E/k_BT}}{\left(e^{\hbar\omega_E/k_BT}-1\right)^2}, \quad (8)$$

Using the approximation $\exp\{\hbar\omega_E/k_BT\} \approx +\infty$, we calculate the anharmonic TE coefficient of Fe in the LT limit $(T \to 0)$ from Eq. (8). The obtained result is:

$$\alpha_T(T) = \frac{81\hbar^2\omega_E^2}{484D\alpha r_0 k_B T^2}\cdot\frac{1}{e^{\hbar\omega_E/k_BT}}, \quad (9)$$

Using the approximation $\exp\{\hbar\omega_E/k_BT\} \approx 1+\hbar\omega_E/k_BT$, we calculate the anharmonic TE coefficient of Fe in the high temperature (HT) limit $(T \to +\infty)$ from Eq. (8). The obtained result is:

$$\alpha_T(T) = \frac{81k_B}{484D\alpha r_0}, \quad (10)$$

A nomenclature of physical symbols is given in Table 1, which reports symbols and their units of measurement together used in these equations. This nomenclature is given for the convenience of following the above equations and calculating the numbers below.

Table 1. The nomenclature of physical symbols.

Physical symbol	Physical meaning	Unit
α_T	TE coefficient	K^{-1}
r	Instantaneous atomic distance	Å
r_0	Equilibrium atomic distance	Å
ℓ	Length	Å
T	Temperature	K
x	Displacement	Å
m	Atomic mass	eV.s^2.Å^{-2}
k_{eff}	Effective force constant	eVÅ^{-2}
k_{an}	Anharmonicity force constant	eVÅ^{-3}
V_{eff}	anharmonic effective potential	eV
α	Width of Morse potential	Å^{-1}
D	Dissociation of Morse potential	eV
ω_E	Correlated Einstein frequency	Hz
θ_E	Correlated Einstein temperature	K
$\hbar$	Reduced Planck constant	eV.s
k_B	Boltzmann constant	eV. Å
$\sigma^{(1)}$	First EXAFS cumulant	Å

Thus, the QACE model has been extended to calculate the anharmonic TE coefficient of Fe efficiently. The obtained expression using this model can satisfy all their temperature-dependent fundamental properties.

III. RESULT AND DISCUSSION

In numerical calculations of Fe, we use the atomic mass $m = 5.788\times10^{-27}$ eV.s^2.Å^{-2} (Ashcroft & Mermin, 1976) and Morse potential parameters $r_0 = 2.845$ Å, $\alpha = 1.3885$ Å^{-1}, $D = 0.4174$ eV (Girifalco & Weizer, 1959) to calculate the correlated Einstein temperature and frequency, the local force constants, the position-dependent AE potential, the temperature-dependent first and TE coefficient. Our obtained results are compared with those obtained using the classical anharmonic correlated Einstein (CACE) model (Tien, 2020b) and experiments (Dunn, 2016; Landsberg, 2018; Hwang, 1972). From these obtained comparisons, we analyse and discuss the efficacy of the QACE model in investigating the anharmonic TE coefficient of Fe.

Using Eqs. (5) and (6) in the QACE model, we have calculated the local force constants $k_{eff} = 2.9506$ eVÅ^{-2} and $k_{an} = -0.8380$ eVÅ^{-3}, the correlated Einstein frequency $\omega_E = 3.1836 \times 10^{13}$ Hz, and the correlated Einstein temperature $\theta_E = 243.1829$ K. Meanwhile, the measured values by Pirog & Nedoseikina (2003) at Synchrotron Radiation Siberian Center (SRSC), Russia obtain the local force constants $k_{eff} = 4.0 \pm 0.5$ eVÅ^{-2} and $k_{an} = -1.7 \pm 0.7$ eVÅ^{-3}, the correlated Einstein frequency $\omega_E = 3.32 \pm 0.29 \times 10^{13}$ Hz, and the correlated Einstein temperature $\theta_E = 253.5 \pm 21.9$ K. It can be seen that our results are suitable with the experimental values (Pirog & Nedoseikina, 2003), especially for the correlated Einstein temperature and frequency.

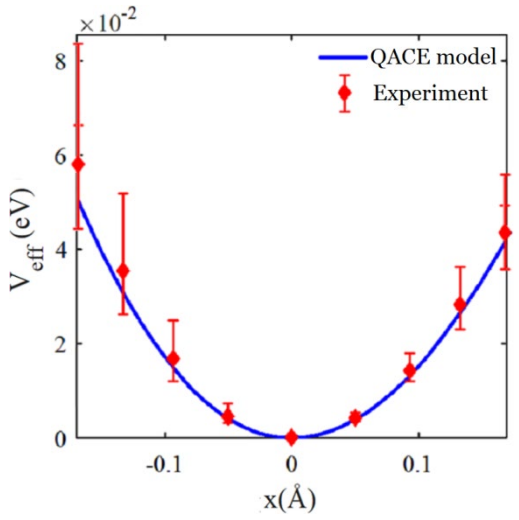

Figure 3. The position-dependent AE potential of Fe obtained using the experiment (Pirog & Nedoseikina, 2003) and the QACE model.

The position dependence of the AE potential of Fe in the position range from −0.17 Å to 0.17 Å is represented in Figure 3. Herein, our obtained result using the QACE is calculated by Eq. (4), and the experimental values are obtained using the Eq. (3) and the measured local force constants. The obtained results show that the graph representing the AE potential is asymmetric, in which the values at the positive positions are smaller than those at the negative positions of the same magnitude.

Table 2. The AE potential of Fe is obtained using the QACE model and experimental data.

Quantity	Value								
x (Å)	- 0.17	- 0.13	- 0.09	-0.05	0	0.05	0.09	0.13	0.17
V_{eff} (eV)[a]	0.09	0.05	0.02	0.01	0	0.01	0.02	0.05	0.08
V_{eff} (eV)[b]	0.12	0.07	0.03	0.01	0	0.01	0.03	0.06	0.11

[a]*Our values are obtained using the QACE model.*

[b]*The average values are obtained from the experimental data determined by Pirog & Nedoseikina (2003).*

The obtained values of the AE potential are given in Table 1. It can be seen that our results agree well with the obtained values from experimental data (Pirog & Nedoseikina, 2003), especially at positions around the equilibrium position $(x = 0)$.

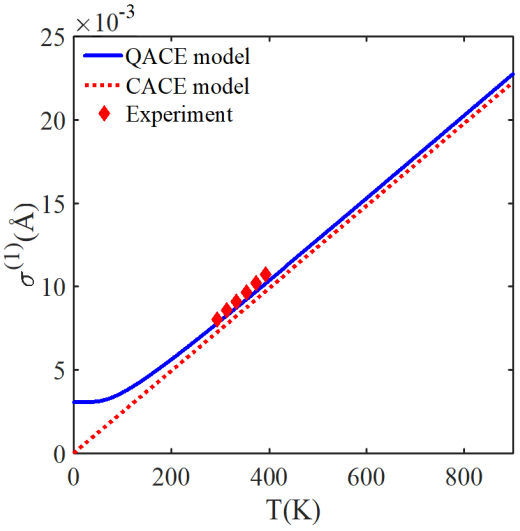

Figure 4. The temperature-dependent first EXAFS cumulant of Fe obtained using the experiment (Pirog & Nedoseikina, 2003) and the CACE (Tien, 2020b) and QACE models.

The temperature dependence of the first EXAFS cumulant $\sigma^{(1)}(T)$ of Fe in a range from 0 to 900 K is represented in Fig. 4. Herein, our obtained result using the QACE model is calculated by Eq. (7), and the obtained result using the CACE model is calculated from the obtained expression by Hung *et al.* (2017b). Meanwhile, the experimental values at 293 K, 313 K, 333 K, 353 K, 373 K, and 393 K are measured by Pirog & Nedoseikina (2003) at the SRSC. It can be seen that our result agrees well with those obtained using the CACE model (only in the HT region) (Tien, 2020b) and experiment (Pirog & Nedoseikina, 2003). For example, the obtained results using the QACE model, CACE model (Tien,

2020b), and experiment (Pirog & Nedoseikina, 2003) at $T = 293$ K are $\sigma^{(1)} = 7.8\times10^{-3}$ Å, $\sigma^{(1)} = 7.2\times10^{-3}$ Å, and $\sigma^{(1)} = 8.0\times10^{-3}$ Å, respectively. Moreover, the CACE model (Tien, 2020b) cannot calculate quantum effects using classical statistical theory because this model cannot work well in the LT region, so it can be seen that the obtained result using the CACE model (Tien, 2020b) approaches zero as the temperature approaches zero.

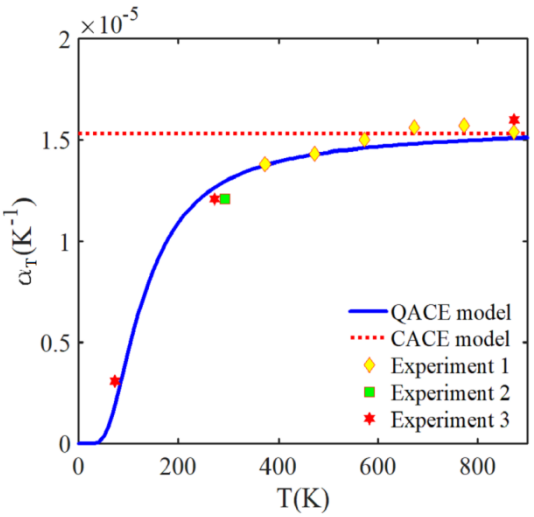

Figure 5. The temperature-dependent TE coefficient of Fe obtained using the CACE (Tien, 2020b) and QACE models and the experiment 1 (Hwang, 1972), experiment 2 (Dunn, 2016), and experiment 3 (Landsberg, 2018).

The temperature dependence of the TE coefficient of Fe in a range from 0 to 900 K is represented in Figure 5. Our obtained result using the QACE model is calculated by Eq. (8), and the obtained result using the CACE model is calculated by Eq. (2) with the obtained first EXAFS cumulant by Hung *et al.* (2017b). Meanwhile, the experimental values are determined by Hwang (1972), Dunn (2016), and Landsberg (2018). Moreover, our result increase with increasing temperature T and approaches those obtained using the CACE model (Tien, 2020b) in the HT limit, which fits perfectly with Eq. (10) and shows that the anharmonic effects can be efficiently described by this QACE model. Meanwhile, the obtained result using the CACE model (Tien, 2020b) is constant because the temperature-dependent first EXAFS cumulant is a linear function in this model, as seen in Figure 4.

Table 3. The TE coefficient of Fe is obtained using the QACE model and experimental data.

Quantity	**Value**								
T (K)	73	273	293	373	473	573	673	773	873
α_T $(\times10^{-5}\mathrm{K}^{-1})$ [a]	0.19	1.26	1.29	1.37	1.43	1.46	1.48	1.50	1.51
α_T $(\times10^{-5}\mathrm{K}^{-1})$ [b]				1.38	1.43	1.50	1.57	1.59	1.55
α_T $(\times10^{-5}\mathrm{K}^{-1})$ [c]			1.21						
α_T $(\times10^{-5}\mathrm{K}^{-1})$ [d]	0.30	1.20							1.60

[a] *Our values are obtained using the QACE model.*
[b] *The values are obtained from the experimental data determined by* Hwang (1972).
[c] *The values are obtained from the experimental data determined by* Dunn (2016).
[d] *The values are obtained from the experimental data determined by* Landsberg (2018).

The obtained values of the TE coefficient are given in Table 3. It can be seen that our result agrees with those obtained from the experimental data, while the obtained value using the CACE model $\alpha \simeq 1.53 \times 10^{-5}\mathrm{K}^{-1}$ is not satisfied with the experimental values in the LT region because the quantum effects are not taken into account in the CACE model.

Thus, the obtained results of the anharmonic TE coefficient using the QACE model agree with those obtained using the experiments and the CACE model in the HT region.

IV. CONCLUSION

In this investigation, we have performed an efficient model to analyse and calculate the anharmonic TE coefficient of Fe. The calculated temperature-dependent TE coefficient using the QACE model can satisfy all of its fundamental properties. The increase of the TE coefficient with increasing temperature T shows that the crystal lattice expands more strongly at higher temperatures. This result can also describe the influence of anharmonic effects in the HT region and the influence of quantum effects in the LT region on the anharmonic TE coefficient.

The good agreement of our results with those obtained using the experiments and the CACE model at various temperatures shows the efficacy of the QACE model in investigating the anharmonic TE coefficient of Fe. The present model can be used to calculate and analyse the anharmonic TE coefficient of other metals in both the LT and HT regions.

V. ACKNOWLEDGEMENT

This investigation was supported by the University of Fire Prevention and Fighting, 243 Khuat Duy Tien, Thanh Xuan, Hanoi, Vietnam.

VI. CONFLICT OF INTEREST

The authors declare that they have no competing financial interests or known personal relationships that could have influenced the work reported in this article.

VII. REFERENCES

Ashcroft, NW & Mermin, ND (eds) 1976, Solid State Physics, 1st edn, Holt-Rinehart & Winston, New York, USA.

Dunn, BD (eds) 2016, Materials and Processes for Spacecraft and High-Reliability Applications, 1st edn, Springer praxis books, New York, USA.

Eisenberger, P & Brown, GS 1979, 'The study of disordered system by EXAFS: Limitations. Solid State Communication', vol. 29, no. 6, pp. 481-484.

Emsley J (eds) 2011, Nature's Building Blocks: An A-Z Guide to the Elements, 2nd edn, Oxford University Press, Oxford, UK.

Fornasini, P, Grisenti, R, Dapiaggi, M, Agostini, G & Miyanaga, T 2017, 'Nearest-neighbour distribution of distances in crystals from extended X-ray absorption fine structure', Journal of Chemical Physics, vol. 147, no. 4, p. 044503.

Girifalco, LA & Weizer, VG 1959, 'Application of the Morse Potential Function to Cubic Metals', Physical Review, vol. 114, no. 3, pp. 687-690.

Ho, CY & Taylor, RE (eds) 1998, Thermal Expansion of Solids, ASM International, Ohio, USA.

Hung, NV & Rehr, JJ 1997, 'Anharmonic correlated Einstein-model Debye-Waller factors', Physical Review B, vol. 56, no. 1, pp. 43-46.

Hung, NV, Thang, CS, Duc, NB, Vuong, DQ & Tien, TS 2017a, 'Temperature Dependence of Theoretical and Experimental Debye-Waller Factors, Thermal Expansion and XAFS of Metallic Zinc', Physica B: Condensed Matter, vol. 521, pp. 198-203.

Hung, NV, Thang, CS, Duc, NB, Vuong, DQ & Tien, TS 2017b, 'Advances in Theoretical and Experimental XAFS Studies of Thermodynamic Properties, Anharmonic Effects and Structural Determination of FCC Crystals', European Physical Journal B, vol. 90, p. 256.

Hwang, JW 1972, 'Thermal expansion of nickel and iron, and the influence of nitrogen on the lattice parameter of iron at the Curie temperature', Master thesis, Missouri University of Science and Technology, Missouri, USA.

Landsberg, GS (eds) 2018, Textbook of Elementary Physics, vol. 2, Aargon Press, New Delhi, India.

Lee, PA, Citrin, PH, Eisenberger, P & Kincaid, BM 1981, 'Extended x-ray absorption fine structure its strengths and limitations as a structural tool. Reviews of Modern Physics', vol. 53, no. 4, pp. 769-806.

Pirog, IV & Nedoseikina, TI 2003, 'Study of effective pair potentials in cubic metals, Physica B, vol. 334, pp. 123-129.

Sevillano, E, Meuth, H & Rehr, JJ 1979, 'Extended x-ray absorption fine structure Debye-Waller factors. I. Monatomic crystals', Physical Review B, vol. 20, no. 12, pp. 4908-4911.

Simon, SH (eds) 2013, The Oxford Solid State Basics, 1st edn, Oxford University Press, Oxford, UK.

Smith, WF & Hashemi, J (eds) 2006, Foundations of Materials Science and Engineering, 4th edn, McGraw-Hill Book, New York, USA.

Stern, EA, Bunker, BA & Heald, SM 1980. 'Many-body effects on extended x-ray absorption fine structure amplitudes', Physical Review B, vol. 21, no. 12, pp. 5521-5539.

Tien, TS 2020a, 'Advances in Studies of the Temperature Dependence of the EXAFS Amplitude and Phase of FCC Crystals', Journal of Physics D: Applied Physics, vol. 53, no. 11, p. 315303.

Tien, TS 2020b, 'Temperature dependence of EXAFS spectra of BCC crystals analyzed based on classical anharmonic correlated Einstein model', Journal of Theoretical and Applied Physics, vol. 14, no. 3, pp. 295-305.

Tien, TS 2022, 'Extending quantum anharmonic correlated Einstein model in studies of anharmonic EXAFS Debye-Waller factor of BCC structure metals', European Physical Journal Plus, vol. 137, p. 1009.

Tien, TS, Thuy, NTM, Lien, VTK, Anh, NTN, Bich, DN & Thanh, LQ 2023, 'Calculation of Temperature-Dependent Thermal Expansion Coefficient of Metal Crystals Based on Using Anharmonic Correlated Debye Model', Advances in Technology Innovation, vol. 8, no. 1, pp. 73-80.

Tröger, L, Yokoyama, T, Arvanitis, D, Lederer, T, Tischer, M & Baberschke, K 1994, 'Determination of bond lengths,

atomic mean-square relative displacements, and local thermal expansion by means of soft-x-ray photoabsorption', Physical Review B, vol. 49, no. 2, pp. 888-903.

Vila, FD, Spencer, JW, Kas, JJ, Rehr, JJ & Bridges, F 2018, 'Extended X-Ray Absorption Fine Structure of ZrW2O8: Theory vs. Experiment. Frontiers in Chemistry', vol. 6, p. 356.

Yokoyama, T 2019, "Chaveanghong S. Anharmonicity in elastic constants and extended x-ray-absorption fine structure cumulants', Physical Review Materials, vol. 3, p. 033607.

Yokoyama, T, Kobayashi, K, Ohta, T & Ugawa, A 1996, 'Anharmonic Interatomic Potentials of Diatomic and Linear Triatomic Molecules Studied by Extended X-Ray Absorption Fine Structure', Physical Review B, vol. 53, no. 10, pp. 6111-6122.